Published in final edited form as:
Hepatology. 2014 September ; 60(3): 941–953. doi:10.1002/hep.27203.

Expansion of PROMININ-1-expressing cells in association with fibrosis of biliary atresia

Nirmala Mavila[1], **David James**[1], **Pranavkumar Shivakumar**[4], **Marie V. Nguyen**[1], **Sarah Utley**[1], **Katrina Mak**[1], **Allison Wu**[1], **Shengmei Zhou**[2], **Larry Wang**[2], **Christopher Vendyres**[1], **Megan Groff**[1], **Kinji Asahina**[3], and **Kasper S Wang**[1]

[1]Developmental Biology, Regenerative Medicine and Stem Cell Program, The Saban Research Institute, Los Angeles, CA

[2]Department of Pathology, Children's Hospital Los Angeles, Los Angeles, CA

[3]Department of Pathology, Keck School of Medicine at the University of Southern California, Cincinnati, OH

[4]Division of Pediatric Gastroenterology, Hepatology and Nutrition, Cincinnati Children's Hospital Medical Center, Cincinnati, OH

Abstract

Biliary atresia (BA), the most common cause of end-stage liver disease and the leading indication for pediatric liver transplantation, is associated with intrahepatic ductular reactions within regions of rapidly expanding periportal biliary fibrosis. While the extent of such biliary fibrosis is a negative predictor of long-term transplant-free survival, the cellular phenotypes involved in the fibrosis are not well established. Using a Rhesus rotavirus (RRV)-induced mouse model of BA, we demonstrate significant expansion of a cell population expressing the putative stem/progenitor cell marker PROMININ-1 (PROM1) adjacent to ductular reactions within regions of periportal fibrosis. PROM1$^{positive\ (pos)}$ cells express *Collagen-1α1*. Subsets of PROM1^{pos} cells co-express progenitor cell marker CD49f, epithelial marker E-CADHERIN, biliary marker CYTOKERATIN-19, and mesenchymal markers VIMENTIN and α-SMOOTH MUSCLE ACTIN. Expansion of the PROM1^{pos} cell population is associated with activation of Fibroblast Growth Factor (FGF) and Transforming Growth Factor-β (TGFβ) signaling. *In vitro* co-treatment of PROM1-expressing *Mat1a*$^{-/-}$ hepatic progenitor cells with recombinant human FGF10 and TGFβ1 promotes morphologic transformation toward a myofibroblastic cell phenotype with increased expression of myofibroblastic genes *Collagen-1α1*, *Fibronectin*, and *α–Smooth muscle actin*. Infants with BA demonstrate similar expansion of periportal PROM1^{pos} cells with activated SMAD3 signaling in association with increased hepatic expression of *FGF10, FGFR1*, and *FGFR2* as well as mesenchymal genes *SLUG* and *SNAIL*. Infants with perinatal subtype of BA have higher tissue levels of *PROM1* expression than those with embryonic subtype.

Please address all correspondences to: Kasper S. Wang, M.D., Children's Hospital Los Angeles, 4650 Sunset Blvd, Mailstop 100, Los Angeles, CA 90027, Office: (323) 361-2338, Fax: (323) 361-3534, kwang@chla.usc.edu.

Conflict of interest: None

Conclusion—Expansion of collagen-producing PROM1^{pos} cells within the regions of periportal fibrosis is associated with activated FGF and TGFβ pathways in both experimental and human BA. PROM1^{pos} cells may, therefore, play an important role in the biliary fibrosis of BA.

Keywords

liver fibrosis; progenitor cells; Rhesus Rotavirus; Prominin-1; biliary atresia

INTRODUCTION

Biliary atresia (BA) is a disease of infants characterized by progressive, fibro-inflammatory obliteration of the extrahepatic biliary tree and rapidly progressing intrahepatic biliary fibrosis. BA is the most common cause of pediatric end-stage liver disease, and if untreated, is inevitably fatal within the first two years of life (1). Primary treatment, which involves surgical drainage of bile, is successful only half of the time (2). Even with successful surgical drainage, the majority of patients with BA still experience progression of intrahepatic biliary fibrosis towards cirrhosis (1). Importantly, transplant-free survival with one's native liver inversely correlates with the extent of intrahepatic fibrosis at the time of surgery (1, 2). Unfortunately, the mechanism of BA-associated fibrosis remains poorly understood.

Infants with BA typically demonstrate extensive intrahepatic biliary ductular reactions within regions of bridging fibrosis, as seen with other obstructive cholangiopathies (3, 4). Within and adjacent to intrahepatic ductular reactions and extrahepatic peribiliary glands are cells that express stem/progenitor cell markers (5, 6). Cholestasis, induced pharmacologically by 3,5-diethoxycarbonyl-1,4-dihydrocollidine (DDC) in rodents, similarly manifests ductular reactions comprised of cells expressing stem/progenitor cell markers (7). Amongst these markers is CD133, also known as PROMININ-1 (PROM1), a penta-transmembrane glycoprotein expressed by stem and cancer stem cells in a variety of organs, including liver (8, 9). The role of these stem/progenitor marker-expressing cells in BA is unclear.

Transdifferentiation of hepatic stellate cells is considered the major source of extracellular matrix-producing myofibroblasts during liver injury and fibrosis (10). There are reports that hepatocytes and cholangiocytes may contribute to liver fibrosis via epithelial-to-mesenchymal transdifferentiation in adult animals (11, 12) although more recent fate tracing studies refute this concept (13, 14). Hepatic progenitor cells (HPC) associated with ductular reactions have been implicated in extracellular matrix deposition although their role is unclear (15). Given that biliary fibrosis associated with ductular reactions is histologically and potentially mechanistically distinct from hepatocyte-specific injury-induced fibrosis, elucidating the origin of cell populations contributing to fibrosis in BA may be critical to intervening with this highly aggressive fibrogenic disease.

In this study, we characterized the expansion of a novel population of PROM1-expressing cells within regions of evolving periportal biliary fibrosis both in a murine model of RRV-infected experimental BA as well as in infants with BA.

MATERIALS AND METHODS

Mouse model of BA

BALB/c mice (Charles River Laboratories) were bred, maintained, and cared for in a manner consistent with criteria outlined in the National Academy of Sciences Guide for the Care and Use of Laboratory Animals and approved by the Institutional Animal Care and Use Committees of Children's Hospital Los Angeles and Cincinnati Children's Hospital Center.

Experimental BA was induced by inoculating newborn BALB/c mouse pups as previously described (16). Serum and liver samples were collected up to 2 weeks post-inoculation after euthanasia. Six-week old, wild-type C57BL/6J male mice (Jackson Laboratories) underwent bile duct ligation, treatment either with carbon tetrachloride (Sigma-Aldrich), or 0.1% DDC diet (Test Diet, Richmond) as previously described (14, 17). *CMV^{cre};Rosa26$^{rtTA/-}$;tet(O)-Fgf10$^{+/-}$* mice and littermate control mice were given water with 1% doxycycline (Clontech) two days prior to and throughout DDC treatment in order to induce *Fgf10* over-expression (17).

Fluorescence Activated Cell Sorting (FACS) Analysis

Liver cell suspensions were collected as previously described (18) one and two weeks after RRV challenge. One million live cells were F_c blocked, incubated with 2 μg of anti-PROM1-Phycoerythrin (eBiosciences, San Diego, CA), and washed with FACS buffer prior to analysis using FACS Calibur (BD Biosciences, San Jose, CA). Compensation was performed using BD™ CompBeads (BD Biosciences). Gating was determined using isotype IgG-stained controls. Flow cytometric analysis was done using Flow-Jo software (Tree Star, Ashland, OR).

Immunofluorescence staining

Livers were fixed in 4% paraformaldehyde (PFA, Poly Sciences Inc., Warrington, PA) and embedded in paraffin for sectioning. Immunofluorescence staining was performed as described previously (9) (Supplemental Table 1). Signals were detected by secondary antibodies conjugated either with anti-mouse Cy3/Cy5, anti-rat Cy3/Cy5, or anti-rabbit Cy3/Cy5 (Jackson Immuno Research Lab, West Grove, PA). Fluorescence images were acquired by an LSM700 confocal system controlled by ZEN software (Carl Zeiss Microimaging, Thornwood, NY) or by a Leica DM5500B immunofluorescence microscope using Leica Suite Advanced Fluorescence (LAS AF) 6000 software (Wetzlar, Germany). Bright field images were acquired using a Leica DM1000 (DFC290) transmitted light microscope (Leica Microsystems, Switzerland) using Leica Application Suite, Version 2.7.1R1.

Western blot analysis

Total protein lysates were prepared and Western blot analyses were performed as previously described (9) (Supplemental Table 1).

Human BA tissue analysis

Human biopsy samples and relevant clinical data were collected from BA patients undergoing Kasai portoenterostomy at CHLA under a study protocol approved by the Institutional Review Board at CHLA, with informed consent obtained from patient's parents. Microarray analysis raw data were obtained from Biliary Atresia Research Consortium database http://genet.cchmc.org (19).

PCR

Total RNA was isolated from snap-frozen human and mouse liver tissues and FACS-sorted cells using the Qiagen RNA isolation kit (Valencia, CA). cDNA synthesis, RTPCR and quantitative real-time PCR (qPCR) were performed as previously described (9) using intron spanning and gene-specific primers (Supplemental Table 2).

Mat1a$^{-/-}$ cell culture

PROM1-expressing *Mat1a*$^{-/-}$ cells were cultured as previously described (9) with recombinant (r) human (h) FGF10 (25 ng/mL) and/or rhTGFβ1 (5 ng/mL).

Determination of tissue fibrosis

Sirius red staining was performed as previously described (17) and quantified densitometrically using Image J software (NIH). The extent of fibrosis and ductular proliferation in human BA liver samples were scored by two clinical pathologists blinded to clinical data and *PROM1* expression levels as previously described (20, 21).

Statistical analysis

Analysis of Variance with post hoc Fisher's Protect Least Significant Difference test was performed using Statview software (SAS Institute Inc., Cary, NC) to calculate statistical significance ($p < 0.05$).

RESULTS

Expansion of PROMININ-1 expressing cells in the periportal fibrotic areas of RRV-infected livers

Two weeks after postnatal day zero (P0) RRV inoculation, mouse pups were jaundiced and excreted acholic stools consistent with BA as previously reported (16). RRV-challenged livers exhibited accumulation of small cells with high nuclear-to-cytoplasmic ratio near the portal vein (Figure 1A) along ductular reactions similar to human BA (Supplemental Figure 1). We observed an increase in the number of PROM1^{pos} cells in the periportal regions of the RRV-infected livers compared to saline controls up to 2 weeks both by immunofluorescence and FACS (Figure 1B-D, Supplemental Figure 2). With P3 RRV injections, pups did not develop cholestasis and there was no increase in PROM1^{pos} cells (Supplemental Figure 3). In P0 RRV-challenged livers, PROM1^{pos} cells emerged predominantly adjacent to the expanding ductular cells expressing CYTOKERATIN-19 (CK19) along the proximal intrahepatic branches of the portal vein and bile ducts (Supplemental Figure 4). To lesser extents, PROM1^{pos} cells were present in adult mouse

models of ductular proliferation and fibrosis three weeks after bile duct ligation and after two weeks of 3,5-diethoxycarbonyl-1,4-dihydrocollidine (DDC) treatment (Supplemental Figure 5B-C) (17); PROM1^{pos} cells were not present in livers after six weeks of carbon tetrachloride exposure (Supplemental Figure 5A) suggesting that the emergence of PROM1^{pos} cells may be unique to biliary-specific injuries.

Infants with BA exhibit some degree of biliary fibrosis ranging from mild periportal fibrosis to cirrhosis marked with bridging fibrosis and hepatocyte loss (3). Overlay of immunofluorescence images with Sirius red staining demonstrated clustered PROM1^{pos} cells adjacent to CK19^{pos} ductular reactions predominantly within nests of new collagen deposition (Figure 2A). PROM1^{pos} cells co-stained positively with Type 1 COLLAGEN (COL1) and FACS-sorted PROM1^{pos} cells expressed *Collagen-1α1*, thus, implicating PROM1^{pos} cells as a source of collagen synthesis in the biliary fibrosis of mice with experimental BA (Figure 2B, B'). Over the 2 weeks following RRV challenge, increases in PROM1^{pos} and COL1^{pos} cells paralleled Sirius red staining and serum bilirubin levels (Figure 2C-F).

PROM1^{pos} cells exhibit dual epithelial-mesenchymal cell characteristics

Two-week RRV-challenged livers exhibited PROM1^{pos} cells that co-expressed CD49f (Figure 3A), a Laminin receptor highly expressed by both epithelial and mesenchymal progenitor cells (22). PROM1^{pos} cells also co-expressed epithelial markers CK19 and E-CADHERIN (Figure 3B-C), but not HEPATOCYTE NUCLEAR FACTOR-4α, suggesting a potential absence of hepatocyte differentiation capacity at this time point (Figure 3D). ~52% of all PROM1^{pos} cells expressed putative portal fibroblast marker, α-SMOOTH MUSCLE ACTIN (αSMA) and a subset of PROM1^{pos} cells co-expressed mesenchymal marker VIMENTIN (Figure 4A, A'). Numerous periportal cells also co-expressed αSMA and E-CADHERIN, αSMA and CK19, or VIMENTIN and CK19 suggesting that PROM1^{pos} cells may be both epithelial and mesenchymal in nature (Figure 4B, B'). PROM1^{pos} cells did not express Fibroblast Specific Protein (FSP1), a marker specific for fibroblasts and activated macrophages in the injured livers (Supplemental Figure 6) (23). Western blot analysis demonstrated a significant increase in E-CADHERIN, N-CADHERIN, VIMENTIN and αSMA expression but not CK19 (Figure 4C-D). Importantly, populations of periportal PROM1^{pos}αSMA^{neg}, PROM1^{pos}αSMA^{pos}, and PROM1^{neg}αSMA^{pos} cells all increased over two weeks post RRV inoculation (Supplemental Figure 7). In parallel, there was an observed increase in cells expressing portal fibroblast marker ELASTIN (24) as well as increased ELASTIN deposition surrounding portal veins after RRV inoculation (Supplemental Figure 8). These observations are consistent with the possibility that some collagen-producing myofibroblasts in the periportal regions of BA livers may derive from PROM1-expressing dual epithelial-mesenchymal cells.

Expansion of the PROM1^{pos} cell population is associated with the activation of Fibroblast Growth Factor and AKT/β-catenin pathways

Approximately 5% of PROM1^{pos} cells were proliferating as assessed by phospho-HISTONE-H3 (pHH3) co-positivity (Figure 5A). Notably, the vast majority of liver cell

proliferation during this stage of RRV-induced liver injury was by PROM1^{pos} cells as most pHH3^{pos} cells also co-expressed PROM1 by immunofluorescence (Figure 5D). PROM1^{pos} cells did not co-localize with the apoptosis marker cleaved CASPASE-3 (Supplemental Figure 9).

Immunofluorescence analysis further demonstrated an increase in the number of periportal PROM1^{pos}FGFR1^{pos} cells (Figure 5B). Nearly 40% of PROM1^{pos} cells co-expressed at least one FGFR, specifically FGFR1; more than 50% FGFR1 expressing cells were co-positive for PROM1 (Figure 5E). By immunohistochemistry, FGFR2 was also present in numerous periportal cells (not shown). Co-staining with pHH3 further demonstrated that ~10% of FGFR1^{pos} cells were proliferating (Figure 5C). Western blot analysis further demonstrated a significant 2.5-fold increase in phospho-FGFR protein levels and, hence, provided evidence for increased FGF signaling activation along with increased expression of FGFR1 and FGFR2 in RRV BA livers compared to controls (Figure 5F). Microarray data available through the Biliary Atresia Research Consortium were analyzed for relative expression of genes encoding *FGFR* and *FGF* ligands in human infants with BA compared to age-matched controls. Significant increases in expression of *FGFR1* and *FGFR2* but not *FGFR3* or *FGFR4* were observed (Supplemental Figure 10A). Of all genes encoding FGF ligands, which bind to FGFR1 and/or FGFR2, only *FGF10* expression was upregulated (Supplemental Figure 10B) while *FGF1, FGF3, FGF7* and *FGF22* were not upregulated. Furthermore, livers from mice with BA demonstrated increased FGF10 expression localized mostly to CK8^{neg} non-epithelial, periportal cells and a few CK8^{pos} ductular cells (Supplemental Figure 11A). Rare FGF10^{pos} cells were co-positive for PROM1, DESMIN or αSMA (Supplemental Figure 11B). FACS-sorted PROM1^{pos} cells expressed *Fgf10* by RTPCR (Supplemental Figure 11C). Doxycycline-induced *Fgf10* overexpression during two weeks of DDC treatment of *Rosa26^{rtTa};tet(o)-Fgf10$^{+/-}$* transgenic mice resulted in an increase in PROM1^{pos} cells adjacent to evolving ductular proliferations not typically seen until later, indicating a role for FGF10 in the emergence of PROM1^{pos} cells (Supplemental Figure 5D) (7).

Seven percent of RRV-induced PROM1^{pos} cells co-stained positively for pSer552-β-CATENIN, the AKT-mediated activated form of β-catenin (Supplemental Figure 12A-B). More than 75% of pSer552-β-CATENIN^{pos} cells were PROM1^{pos}. More than 90% of pSer552-β-CATENIN^{pos} cells co-expressed pHH3 and all proliferating cells were co-positive for pSer552-β-CATENIN, thus, linking this pathway in proliferating PROM1-expressing cells during RRV injury. Co-expression of FGFR1 and pSer552-β-CATENIN further demonstrated a link between these two signaling pathways in RRV BA livers in some cells (Supplemental Figure 12A). Western blot analysis further demonstrated significant activation of AKT and β-catenin pathways but not ERK pathway, another downstream mediator of FGFR signaling in RRV-challenged livers (Supplemental Figure 12C-D). Thus, we conclude that while a large percentage of PROM1^{pos} cells co-express FGFR, only a small fraction of PROM1^{pos} cells are proliferating via FGF-induced AKT-mediated β-catenin pathway activation.

TGFβ signaling is activated in PROM1 expressing cells in BA

Several studies have demonstrated increased expression of TGFβ in the livers from patients with BA specifically in ductular reactions and surrounding inflammatory cells (25). By immunofluorescence, we identified an increased number of cells positive for pSMAD3, indicating TGFβ activation, adjacent to ductular reactions in RRV BA livers compared to saline controls. 65% of PROM1^{pos} cells were pSMAD3^{pos} (Figures 6A). A subset of pSMAD3^{pos} cells also expressed VIMENTIN (not shown). Western blot analysis revealed a three-fold increase in pSMAD3 levels with a concurrent decrease in total SMAD3 levels in RRV BA liver compared to saline controls (Figure 6B). There was also increased expression of two transcriptions factors associated with TGFβ signaling activation, SLUG by Western blot analysis and *Snail* by qPCR (26, 27) in RRV BA livers (Figure 6C).

To determine if FGF10 and TGFβ1 promote myofibroblastic differentiation of PROM1^{pos} cells, *in vitro* experiments were performed using *Mat1a*$^{-/-}$ cells, an established transformed murine HPC line that expresses PROM1 along with multiple epithelial and mesenchymal genes (9). Untreated *Mat1a*$^{-/-}$ cells exhibited round, epithelioid morphology and expressed CK19 but only minimal or no VIMENTIN or pSMAD3 (Figure 7A). Treatment with recombinant (r) human (h) FGF10 had no observable effect. In contrast, treatment with rhTGFβ1 induced transformation to a spindle-shaped, fibroblastic morphology with increased VIMENTIN and pSMAD3 cell positivity as well as increases in α*Sma*, *Collagen1*α*1*, and *Fibronectin* expression by qPCR analysis (Figure 7B). Co-treatment with rhFGF10 and rhTGFβ1 resulted in a three-fold augmentation in *Collagen1*α*1* expression compared to rhTGFβ1 alone, indicating a synergism between FGF and TGFβ signaling. We, thus, surmise that the majority of FGFR signaling activation in PROM1^{pos} cells may potentiate the effects of TGFβ pathway activation rather than promotes cell proliferation. While there was evidence of myofibroblastic transdifferentiation with TGFβ pathway activation, there was yet a clear retention of CK19 expression, implying a potential dual epithelial-mesenchymal phenotype.

Infant BA livers demonstrated periportal pSMAD3 activation in both PROM1^{pos} and VIMENTIN^{pos} cells (Figure 8A). Both Western blot and qPCR analyses demonstrated significant upregulation of *PROM1* expression in BA livers compared to normal controls (Figure 8B,C). Microarray analysis of infant BA livers demonstrated greatest fold increases in expression of *PROM1* in comparison to other putative progenitor genes including *CD49f*, *SCA1*, *CD117*, and *CD34* (Supplemental Figure 13). *SLUG* and *SNAIL* were significantly upregulated in BA livers compared to control livers (Figure 8D). Sirius red staining demonstrated a more than 40-fold increase in collagen deposition in BA livers compared to control (Figure 8E). In summary, these data demonstrate an association between expansion of the PROM1^{pos} cell population and TGFβ signaling activation in human BA.

Correlation between PROM1 expression and fibrosis in BA livers

We next sought to determine if there was a definable relationship between *PROM1* expression and any clinical parameters in human BA. Data from eight patients, four of whom experienced successful biliary drainage following Kasai portoenterostomy (total bilirubin below 1.5 mg/dL within the first three months postoperatively (2)) and four of

whom did not establish bile drainage, were reviewed (Supplemental Figure 14A). No trends were observed between *PROM1* levels and Ishak fibrosis or ductular proliferation scores (Supplemental Figure 14B). There was, however, a trend toward higher *PROM1* levels in infants with failed surgical drainage post-Kasai (7.5 ± 6.2 vs. 4.5 ± 2.5, respectively) in this underpowered patient cohort compared to those who had successful surgical drainage. The two patients with the highest total bilirubin levels in the cohort (11 and 13.4 mg/dL) also exhibited the highest relative levels of *PROM1* expression (linear regression analysis R^2 = 0.799). Finally, when subdivided based on age at onset of jaundice, infants with embryonic subtype of BA (at or within two weeks of birth) exhibited significantly lower *PROM1* expression levels compared to infants with perinatal subtype (later than two weeks of age) at 3.4±1.2 versus 10.3±2.7, respectively ($p<0.05$) (Supplemental Figure 14C).

DISCUSSION

In this study, we demonstrate the expansion of a novel population of $PROM1^{pos}$ cells in various models of ductular proliferation-associated biliary fibrosis, and particularly RRV-induced BA. Within the regions of periportal fibrosis in experimental BA, subsets of $PROM1^{pos}$ cells co-express epithelial markers, mesenchymal markers, and Type 1 Collagen. There is a concurrent increase in $PROM1^{pos}\alpha SMA^{pos}$ and $PROM1^{neg}\alpha SMA^{pos}$ cells as well as in $PROM1^{neg}ELASTIN^{pos}$ portal fibroblast cells, which collectively may represent an evolving myofibroblast population. The expansion of $PROM1^{pos}$ cells is associated with FGF signaling activation, in part via periportal FGF10 expression. Additionally, a subset of $PROM1^{pos}$ cells exhibit evidence of activated profibrogenic TGFβ signaling with pSMAD3 expression in association with increased expression of SLUG and *Snail*, which further supports the potential role of PROM1-expressing cells in driving fibrosis in BA. Furthermore, FGF and TGFβ signaling activation promote myofibroblastic differentiation of PROM1-expressing HPCs *in vitro* with induced expression of *Col1α1*. Infants with BA exhibit similar $PROM1^{pos}$ cell expansion in association with FGF and TGFβ signaling activation. Finally, infants with embryonic subtype of BA had lower levels of *PROM1* expression compared to those with perinatal subtype. Thus, we propose that subset of $PROM1^{pos}$ cells undergoes FGF/TGFβ-mediated differentiation to collagen producing cells during BA.

Diseases marked with ductular reactions, such as BA, have been associated with expansion of HPCs (6). In turn, ductular reactions and HPCs have been implicated in liver fibrogenesis (15, 28, 29) although their precise roles have remained unclear. Using a choline-deficient, ethionine-supplemented model of chronic liver injury, Van Hul *et al*. demonstrated that the deposition of collagen preceded the emergence of $CK19^{pos}$ ductular reactions and upregulation of *Cd49f, E-cadherin*, and α-*Fetoprotein* expression suggesting that matrix deposition is independent of HPC expansion (30). The authors, however, did not exclude the possibility that progenitor cells may still contribute to production and deposition of the extracellular matrix. Ding *et al.*, demonstrated that HPC cell lines LE/6 and WB-F344 secrete Connective Tissue Growth Factor (CTGF), a profibrogenic extracellular matrix protein, in response to TGFβ, albeit *in vitro* (31). While our study was too underpowered for linking relative levels of *PROM1* expression with degree of fibrosis, we were, nonetheless, able to establish some clear associations. Infants with perinatal subtype of BA had higher

relative levels of *PROM1* expression than those with embryonic subtype. The perinatal BA subtype is theorized to be more associated with postnatal exposure to fibroinflammatory infectious agents or toxins whereas the embryonic subtype is more associated with congenital malformations and, therefore, thought more likely to be due to dysregulation of biliary organogenesis (32). Prominent ductular reactions and periportal fibrosis were observed in experimental BA, similar to that of BA in human infants. The emergence of PROM1^{pos} cells paralleled the deposition of fibrosis in experimental BA. In addition, the co-localization of PROM1 with COL1 in cells within regions of newly deposited fibrosis along with the expression of *Col1α1* by FACS-sorted PROM1^{pos} cells strongly implicates PROM1^{pos} cells as a source of collagen deposition in BA. During the early stages of hepatogenesis, PROM1^{pos} progenitor cells are more abundant than shortly after birth indicating either cellular attrition or loss of PROM1 expression (33). Within two weeks after RRV challenge, there is a clear re-emergence of PROM1^{pos} cells. Half of all RRV-induced PROM1^{pos} cells express αSMA, indicating a periportal myofibroblastic phenotype. Moreover, over time there is an increase in both PROM1^{pos}αSMA^{pos} and PROM1^{neg}αSMA^{pos} portal myofibroblast as well as an increase in ELASTIN-expressing portal fibroblast cells in RRV BA livers. Elastin fibers, which are normally present surrounding portal veins, increase during liver fibrosis (34, 35).

It is unclear if PROM1^{neg} αSMA^{pos} cells represent a distinct and separate cell lineage from PROM1^{pos}αSMA^{pos} cells. Our data are consistent with previous lineage tracing studies, which demonstrate that neither hepatocytes nor cholangiocytes undergo epithelial-mesenchymal transdifferentiation to myofibroblasts (13, 14). PROM1-expressing cells phenotypically are neither hepatocytes nor cholangiocytes. To determine if a portal myofibroblasts derive in part from PROM1-expressing cells, lineage tracing experiments are planned but not within the scope of this report due to the necessary extensive back-crossing of existing transgenic mice into the requisite BALB/c background (36). Nevertheless, our data are consistent with the possibility that subsets of emerging PROM1^{pos} cells during RRV-induced BA may give rise to collagen-producing portal myofibroblasts. Moreover, PROM1^{pos} cells could also potentially give rise to the adjacent biliary ductular reactions.

We previously demonstrated that the expansion and survival of PROM1^{pos} embryonic HPCs is partially regulated by FGF/AKT/β-catenin pathway activation (9). In this study, only a small fraction of PROM1^{pos} cells exhibit FGF/AKT/β-catenin-mediated proliferation. In RRV BA livers, we show expression of FGF10 in periportal regions as well as evidence of FGFR/AKT/β-catenin pathway activation in some PROM1^{pos} cells, and in human BA, *FGF10* is the only FGFR1/2 ligand encoding gene which is upregulated. The enhanced expansion of PROM1^{pos} cells with FGF10 overexpression during acute DDC injury further supports the role of this pathway in BA. Consistent with previous reports (25), our data also indicate significant TGFβ pathway activation in both experimental BA as well as in human BA. RRV is known to have high tropism for biliary epithelium, causing its initial destruction (16, 37, 38) and the subsequent release of numerous cytokines including TGFβ (39, 40). Although there are multiple potential sources of TGFβ during injury and inflammation, biliary-derived TGFβ likely drives the myofibroblastic differentiation of adjacent PROM1^{pos} cells. Shirakihara *et al.* demonstrated that activation of TGFβ signaling induces

myofibroblastic differentiation of epithelial cells *in vitro* partly due to isoform switching from epithelial *Fgfr2IIIb* to mesenchymal *Fgfr1IIIc* making the cells responsive to FGF2 (41). Harada *et al.* demonstrated similar observations in cultured biliary epithelial cells (42). Ding *et al.* showed evidence of myofibroblastic differentiation of cultured HPCs with TGFβ (31). Our *in vitro* gain-of-function data demonstrate a potential synergism between FGF and TGFβ signaling in the myofibroblastic differentiation of HPCs *in vitro*. Given evidence of FGF and TGFβ signaling activation in PROM1-expressing cells, it is likely that these pathways synergistically promote fibrogenesis in BA.

In summary, we demonstrate a potential functional linkage between the expansion of a PROM1-expressing cell population and the newly evolving fibrosis associated with BA mediated by FGF and TGFβ signaling. Defining the nature of these cells and the factors regulating their cell fate determinations could ultimately lead to novel therapeutic interventions against the fibrosis of BA.

Supplementary Material

Refer to Web version on PubMed Central for supplementary material.

Acknowledgments

We thank Dr. Esteban Fernandez (Imaging core), Dr. Ann George, Mr. Jonathan Kirzner (FACS core) for their help with confocal imaging and FACS analysis respectively. We also thank Dr. Joshua Friedman (University of Pennsylvania) and Dr. Linheng Li (Stower's Institute) for their generous gifts of antibodies to perform this study. We thank Dr. Grace Aldrovandi and William Decker for their assistance with RRV culturing. We thank Cat Goodhue for manuscript review and editing. We would also like to thank Drs. Nanda Kerkar and David Warburton for their stimulating feedback on this project. We thank Dr. Henri R. Ford for his support for this project.

Financial support:

This study was supported in part by the National Institutes of Health Grants K08 AAA01690, U01 DK084538-01, and a CHLA-TSRI core utilization grant (KW) and R01 AA020753 (KA). P.S. is supported by an American Liver Foundation Liver Scholar award. K.M. was supported by California Institute for Regenerative Medicine (CIRM) internship.

Abbreviations

RRV	Rhesus Rotavirus
BA	Biliary Atresia
PROM1	PROMININ-1
TGF	Transforming Growth factor
FGF	Fibroblast growth factor
DMEM	Dulbecco's Modified Eagle Medium
ECM	Extracellular Matrix
FACS	Fluorescence Activated Cell Sorting

REFERENCES

1. Sokol RJ. Corticosteroid treatment in biliary atresia: Tonic or toast? Hepatology. 2007; 46:1675–1678. [PubMed: 18046714]
2. Superina R, Magee JC, Brandt ML, Healey PJ, Tiao G, Ryckman F, Karrer FM, et al. The anatomic pattern of biliary atresia identified at time of Kasai hepatoportoenterostomy and early postoperative clearance of jaundice are significant predictors of transplant-free survival. Ann Surg. 2011; 254:577–585. [PubMed: 21869674]
3. Desmet VJ. Ductal plates in hepatic ductular reactions. Hypothesis and implications. I. Types of ductular reaction reconsidered. Virchows Arch. 2011; 458:251–259. [PubMed: 21287200]
4. Gouw AS, Clouston AD, Theise ND. Ductular reactions in human liver: diversity at the interface. Hepatology. 2011; 54:1853–1863. [PubMed: 21983984]
5. Dipaola F, Shivakumar P, Pfister J, Walters S, Sabla G, Bezerra JA. Identification of intramural epithelial networks linked to peribiliary glands that express progenitor cell markers and proliferate after injury in mice. Hepatology. 2013; 58:1486–1496. [PubMed: 23703727]
6. Stamp LA, Braxton DR, Wu J, Akopian V, Hasegawa K, Chandrasoma PT, Hawes SM, et al. The GCTM-5 epitope associated with the mucin-like glycoprotein FCGBP marks progenitor cells in tissues of endodermal origin. Stem Cells. 2012; 30:1999–2009. [PubMed: 22761039]
7. Rountree CB, Barsky L, Ge S, Zhu J, Senadheera S, Crooks GM. A CD133-expressing murine liver oval cell population with bilineage potential. Stem Cells. 2007; 25:2419–2429. [PubMed: 17585168]
8. Zhu L, Gibson P, Currle DS, Tong Y, Richardson RJ, Bayazitov IT, Poppleton H, et al. Prominin 1 marks intestinal stem cells that are susceptible to neoplastic transformation. Nature. 2009; 457:603–607. [PubMed: 19092805]
9. Mavila N, James D, Utley S, Cu N, Coblens O, Mak K, Rountree CB, et al. Fibroblast growth factor receptor-mediated activation of AKT-beta-catenin-CBP pathway regulates survival and proliferation of murine hepatoblasts and hepatic tumor initiating stem cells. PLoS One. 2012; 7:e50401. [PubMed: 23308088]
10. Mederacke I, Hsu CC, Troeger JS, Huebener P, Mu X, Dapito DH, Pradere JP, et al. Fate tracing reveals hepatic stellate cells as dominant contributors to liver fibrosis independent of its aetiology. Nat Commun. 2013; 4:2823. [PubMed: 24264436]
11. Omenetti A, Bass LM, Anders RA, Clemente MG, Francis H, Guy CD, McCall S, et al. Hedgehog activity, epithelial-mesenchymal transitions, and biliary dysmorphogenesis in biliary atresia. Hepatology. 2011; 53:1246–1258. [PubMed: 21480329]
12. Zeisberg M, Yang C, Martino M, Duncan MB, Rieder F, Tanjore H, Kalluri R. Fibroblasts derive from hepatocytes in liver fibrosis via epithelial to mesenchymal transition. J Biol Chem. 2007; 282:23337–23347. [PubMed: 17562716]
13. Chu AS, Diaz R, Hui JJ, Yanger K, Zong Y, Alpini G, Stanger BZ, et al. Lineage tracing demonstrates no evidence of cholangiocyte epithelial-to-mesenchymal transition in murine models of hepatic fibrosis. Hepatology. 2011; 53:1685–1695. [PubMed: 21520179]
14. Scholten D, Osterreicher CH, Scholten A, Iwaisako K, Gu G, Brenner DA, Kisseleva T. Genetic labeling does not detect epithelial-to-mesenchymal transition of cholangiocytes in liver fibrosis in mice. Gastroenterology. 2010; 139:987–998. [PubMed: 20546735]
15. Williams MJ, Clouston AD, Forbes SJ. Links between hepatic fibrosis, ductular reaction, and progenitor cell expansion. Gastroenterology. 2014; 146:349–356. [PubMed: 24315991]
16. Shivakumar P, Campbell KM, Sabla GE, Miethke A, Tiao G, McNeal MM, Ward RL, et al. Obstruction of extrahepatic bile ducts by lymphocytes is regulated by IFN-gamma in experimental biliary atresia. J Clin Invest. 2004; 114:322–329. [PubMed: 15286798]
17. Utley S, James D, Mavila N, Nguyen MV, Vendryes C, Salisbury SM, Phan J, et al. Fibroblast Growth Factor signaling regulates the expansion of A6-expressing hepatocytes in association with AKT-dependent β-catenin activation. Journal of Hepatology. 2014; 60:1002–1009. [PubMed: 24365171]

18. Berg T, Rountree CB, Lee L, Estrada J, Sala FG, Choe A, Veltmaat JM, et al. Fibroblast growth factor 10 is critical for liver growth during embryogenesis and controls hepatoblast survival via beta-catenin activation. Hepatology. 2007; 46:1187–1197. [PubMed: 17668871]
19. Moyer K, Kaimal V, Pacheco C, Mourya R, Xu H, Shivakumar P, Chakraborty R, et al. Staging of biliary atresia at diagnosis by molecular profiling of the liver. Genome Med. 2010; 2:33. [PubMed: 20465800]
20. Knodell RG, Ishak KG, Black WC, Chen TS, Craig R, Kaplowitz N, Kiernan TW, et al. Formulation and application of a numerical scoring system for assessing histological activity in asymptomatic chronic active hepatitis. Hepatology. 1981; 1:431–435. [PubMed: 7308988]
21. Lee WS, Looi LM. Usefulness of a scoring system in the interpretation of histology in neonatal cholestasis. World J Gastroenterol. 2009; 15:5326–5333. [PubMed: 19908342]
22. Ramalho-Santos M, Yoon S, Matsuzaki Y, Mulligan RC, Melton DA. "Stemness": transcriptional profiling of embryonic and adult stem cells. Science. 2002; 298:597–600. [PubMed: 12228720]
23. Osterreicher CH, Penz-Osterreicher M, Grivennikov SI, Guma M, Koltsova EK, Datz C, Sasik R, et al. Fibroblast-specific protein 1 identifies an inflammatory subpopulation of macrophages in the liver. Proc Natl Acad Sci U S A. 2011; 108:308–313. [PubMed: 21173249]
24. Tuchweber B, Desmouliere A, Bochaton-Piallat ML, Rubbia-Brandt L, Gabbiani G. Proliferation and phenotypic modulation of portal fibroblasts in the early stages of cholestatic fibrosis in the rat. Lab Invest. 1996; 74:265–278. [PubMed: 8569191]
25. Nadler EP, Patterson D, Violette S, Weinreb P, Lewis M, Magid MS, Greco MA. Integrin alphavbeta6 and mediators of extracellular matrix deposition are up-regulated in experimental biliary atresia. J Surg Res. 2009; 154:21–29. [PubMed: 19084240]
26. Dhasarathy A, Phadke D, Mav D, Shah RR, Wade PA. The transcription factors Snail and Slug activate the transforming growth factor-beta signaling pathway in breast cancer. PLoS One. 2011; 6:e26514. [PubMed: 22028892]
27. Herfs M, Hubert P, Kholod N, Caberg JH, Gilles C, Berx G, Savagner P, et al. Transforming agrowth factor-beta1-mediated Slug and Snail transcription factor up-regulation reduces the density of Langerhans cells in epithelial metaplasia by affecting E-cadherin expression. Am J Pathol. 2008; 172:1391–1402. [PubMed: 18385519]
28. Clouston AD, Powell EE, Walsh MJ, Richardson MM, Demetris AJ, Jonsson JR. Fibrosis correlates with a ductular reaction in hepatitis C: roles of impaired replication, progenitor cells and steatosis. Hepatology. 2005; 41:809–818. [PubMed: 15793848]
29. Richardson MM, Jonsson JR, Powell EE, Brunt EM, Neuschwander-Tetri BA, Bhathal PS, Dixon JB, et al. Progressive fibrosis in nonalcoholic steatohepatitis: association with altered regeneration and a ductular reaction. Gastroenterology. 2007; 133:80–90. [PubMed: 17631134]
30. Van Hul NK, Abarca-Quinones J, Sempoux C, Horsmans Y, Leclercq IA. Relation between liver progenitor cell expansion and extracellular matrix deposition in a CDE-induced murine model of chronic liver injury. Hepatology. 2009; 49:1625–1635. [PubMed: 19296469]
31. Ding ZY, Jin GN, Liang HF, Wang W, Chen WX, Datta PK, Zhang MZ, et al. Transforming growth factor beta induces expression of connective tissue growth factor in hepatic progenitor cells through Smad independent signaling. Cell Signal. 2013; 25:1981–1992. [PubMed: 23727026]
32. Sokol RJ, Mack C, Narkewicz MR, Karrer FM. Pathogenesis and outcome of biliary atresia: current concepts. J Pediatr Gastroenterol Nutr. 2003; 37:4–21. [PubMed: 12827000]
33. Schievenbusch S, Sauer E, Curth HM, Schulte S, Demir M, Toex U, Goeser T, et al. Neighbor of Punc E 11: expression pattern of the new hepatic stem/progenitor cell marker during murine liver development. Stem Cells Dev. 2012; 21:2656–2666. [PubMed: 22497843]
34. Pellicoro A, Aucott RL, Ramachandran P, Robson AJ, Fallowfield JA, Snowdon VK, Hartland SN, et al. Elastin accumulation is regulated at the level of degradation by macrophage metalloelastase (MMP-12) during experimental liver fibrosis. Hepatology. 2012; 55:1965–1975. [PubMed: 22223197]
35. Dranoff JA, Wells RG. Portal fibroblasts: Underappreciated mediators of biliary fibrosis. Hepatology. 2010; 51:1438–1444. [PubMed: 20209607]

36. Petersen C, Kuske M, Bruns E, Biermanns D, Wussow PV, Mildenberger H. Progress in developing animal models for biliary atresia. Eur J Pediatr Surg. 1998; 8:137–141. [PubMed: 9676394]

37. Shivakumar P, Sabla GE, Whitington P, Chougnet CA, Bezerra JA. Neonatal NK cells target the mouse duct epithelium via Nkg2d and drive tissue-specific injury in experimental biliary atresia. J Clin Invest. 2009; 119:2281–2290. [PubMed: 19662681]

38. Coots A, Donnelly B, Mohanty SK, McNeal M, Sestak K, Tiao G. Rotavirus infection of human cholangiocytes parallels the murine model of biliary atresia. J Surg Res. 2012; 2:275–281. [PubMed: 22785360]

39. Lamireau T, Le Bail B, Boussarie L, Fabre M, Vergnes P, Bernard O, Gautier F, et al. Expression of collagens type I and IV, osteonectin and transforming growth factor beta-1 (TGFbeta1) in biliary atresia and paucity of intrahepatic bile ducts during infancy. J Hepatol. 1999; 31:248–255. [PubMed: 10453937]

40. Jafri M, Donnelly B, Bondoc A, Allen S, Tiao G. Cholangiocyte secretion of chemokines in experimental biliary atresia. J Pediatr Surg. 2009; 44:500–507. [PubMed: 19302848]

41. Shirakihara T, Horiguchi K, Miyazawa K, Ehata S, Shibata T, Morita I, Miyazono K, et al. TGF-beta regulates isoform switching of FGF receptors and epithelial-mesenchymal transition. EMBO J. 2011; 30:783–795. [PubMed: 21224849]

42. Harada K, Sato Y, Ikeda H, Isse K, Ozaki S, Enomae M, Ohama K, et al. Epithelial-mesenchymal transition induced by biliary innate immunity contributes to the sclerosing cholangiopathy of biliary atresia. J Pathol. 2009; 217:654–664. [PubMed: 19116990]

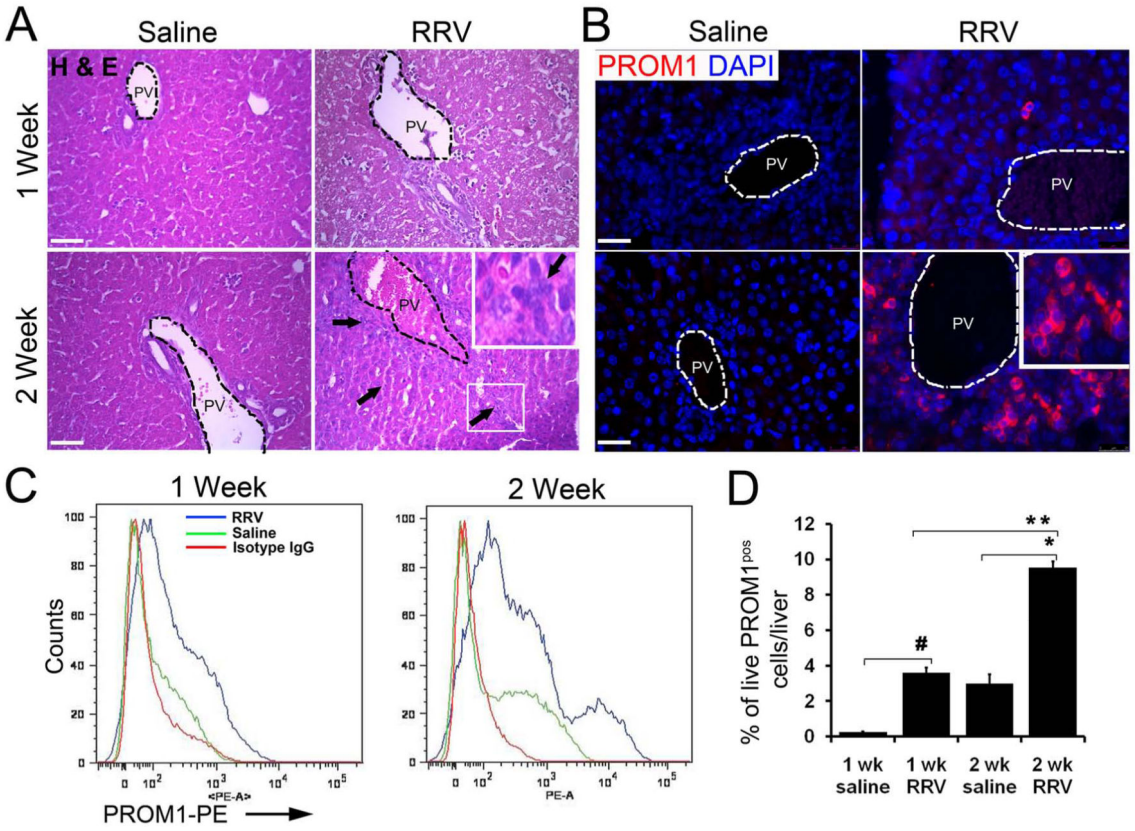

Figure 1.

Expansion of the PROM1-expressing cell population around the periportal regions of RRV BA livers. (A) Hematoxylin and Eosin (H&E) staining on livers from 1 and 2 week saline and RRV infected livers. Arrows indicate new small cells with high nuclear-to-cytoplasmic ratio. (B) Immunofluorescence staining for PROM1 on 1 and 2 week RRV-infected and saline control livers. PV: Portal Vein. (C, D) FACS analysis on 1 and 2 week RRV-infected and saline livers. Percentage of live PROM1^{pos} cells compared between 1 and 2 week RRV as well as with saline controls. Nuclei were stained with DAPI. n=4-6, #p<0.0001, * p< 0.0001, ** p<0.001. Scale bar=25μm.

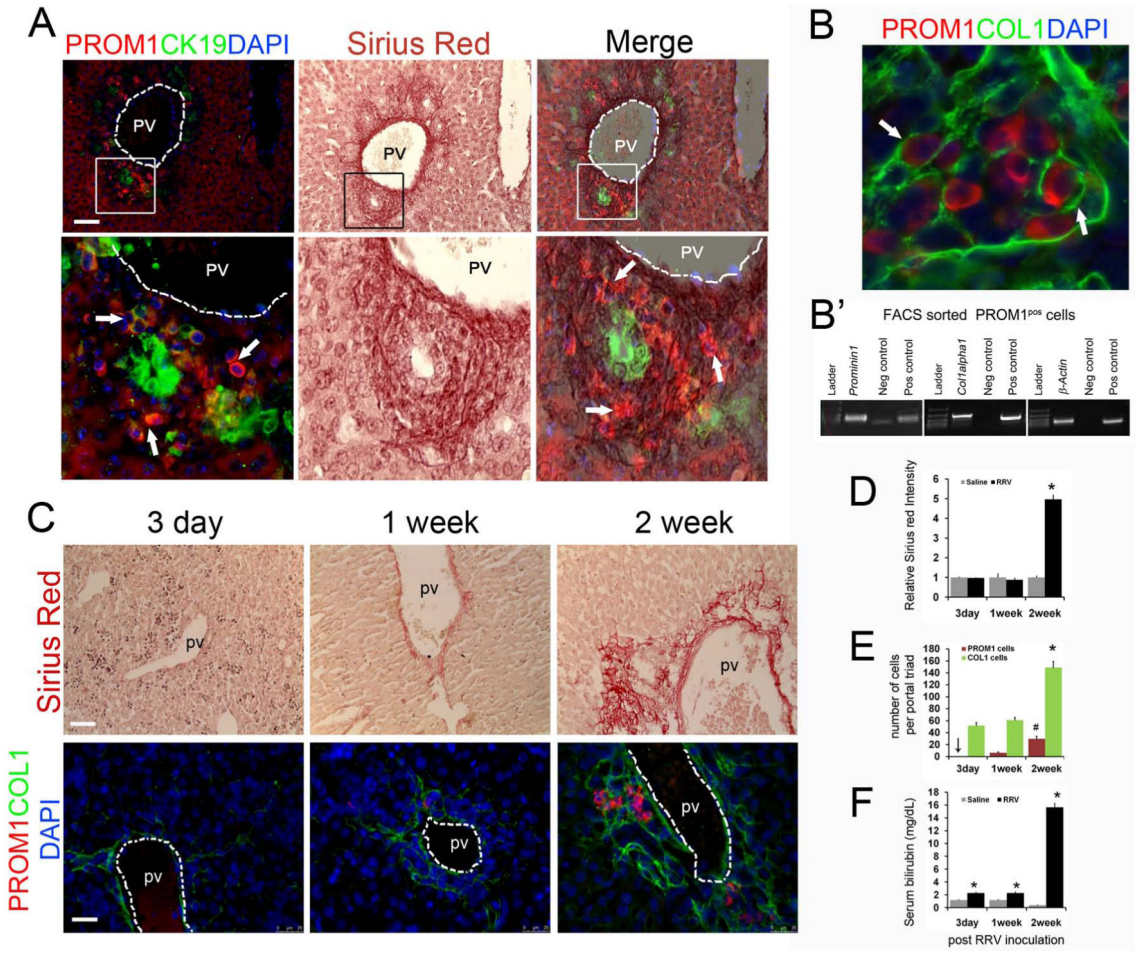

Figure 2.

PROM1 cells are present within the fibrotic periportal areas in RRV BA livers: (A) Immunofluorescence staining for PROM1 and CK19. The same tissue sections were then processed for Sirius Red staining and the two images merged into one. Arrows indicate PROM1^{pos} cells within the collagen deposited areas. (B) High-powered confocal immunofluorescence image of PROM1 and COL1 on 2-week RRV BA liver. (B') RNA was isolated from FACS-sorted PROM1^{pos} cells from 2-week RRV liver tissues and RTPCR was performed to show co-expression of *Prominin1*, *Col1α1* and *βactin.* (C) Expansion of the PROM1^{pos} cell population is associated with increased periportal fibrosis and biliary obstruction after RRV infection. Sirius Red staining for fibrosis and immunofluorescence staining for PROM1 and COL1 on 3-day, 1-week and 2-week post RRV liver. (D) Intensity of Sirius Red staining was quantified using ImageJ (NIH) software, normalized and compared to respective saline controls. Data represented as relative fold increase in intensity. 4-5 20x images were quantified and average value was taken for each liver sample (n=3-4, * p<0.0001 vs. 2 week saline). (E) Quantification of PROM1 and COL1 expressing cells in livers after 3-day, 1-week and 2-week RRV infection. PROM1^{pos} cells and COL1^{pos} cells were counted from 6-8 40× images per sample and mean value was taken for each liver tissue (n= 3-4, p #< 0.005 vs 1 week, p * < 0.001 vs. 3-day and 1-week). (F) Serum bilirubin

levels in RRV infected mice (n=4-6, * $p < 0.0005$ compared to respective saline controls). PV=portal vein, scale bar=25μm.

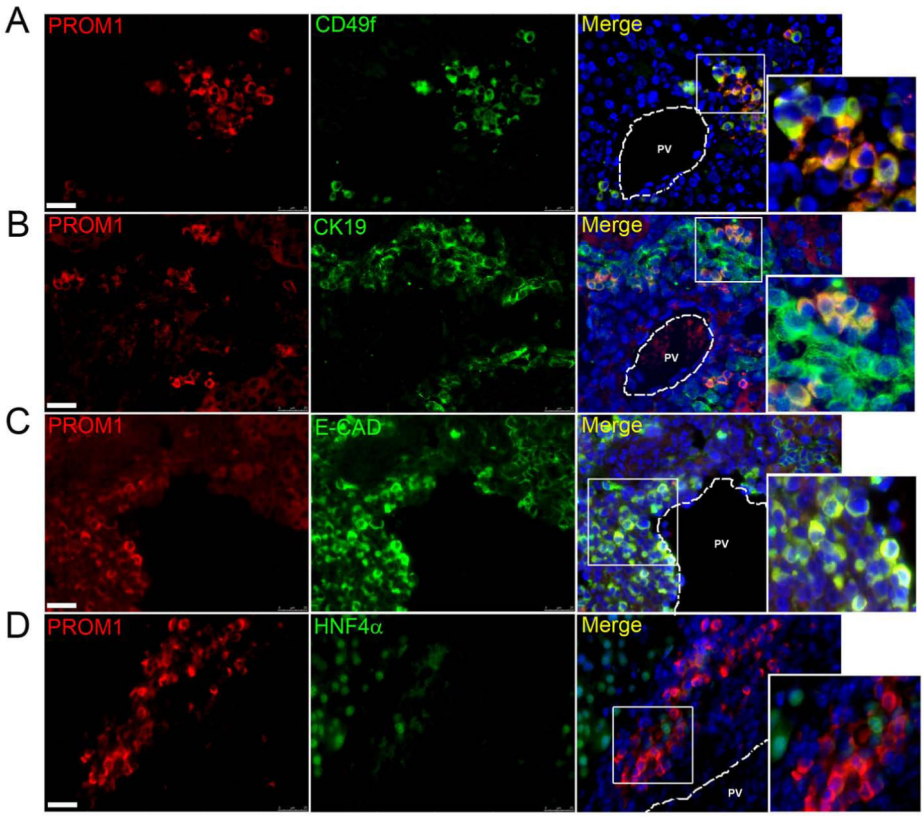

Figure 3.

PROM1^{pos} cells exhibit less differentiated non-hepatocyte epithelial cellular phenotype. Immunofluorescence colocalization of PROM1 in livers from 2-week RRV-infected pups with (A) progenitor cell marker, CD49f, (B) biliary epithelial marker, CK19, (C) epithelial marker, E-CADHERIN (E-CAD), and (D) hepatocyte marker HNF4α. Nuclei were stained with DAPI. Images represent four or more independent staining. Scale bar =25μm, PV= portal vein.

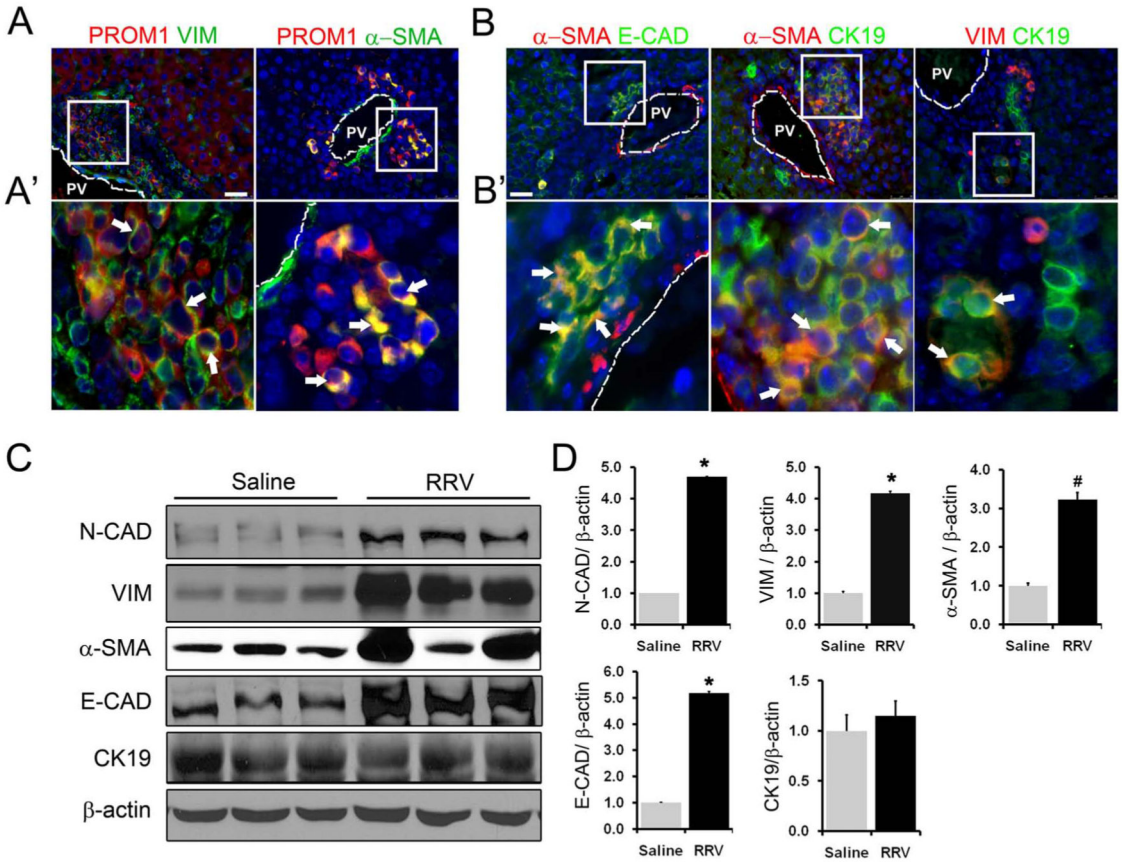

Figure 4.

Increased expression of mesenchymal markers in RRV BA livers (A, A'). PROM1 cells exhibit mesenchymal characteristics with the co-expression of VIMENTIN (VIM) and αSMOOTH MUSCLE ACTIN (αSMA). (B, B') Co-expression of epithelial markers (E-CAD, CK19) with mesenchymal markers (αSMA, VIM) in RRV BA livers. Nuclei were stained with DAPI. Arrows indicate cells co-positive cells in each panel. PV=portal vein, Scale bar=25μm. (C) Western blot analysis of whole liver protein expression from 2-week saline control and RRV BA livers. (D) Densitometric quantification of Western blot data. n=3-4, *p<0.001, # p<0.05.

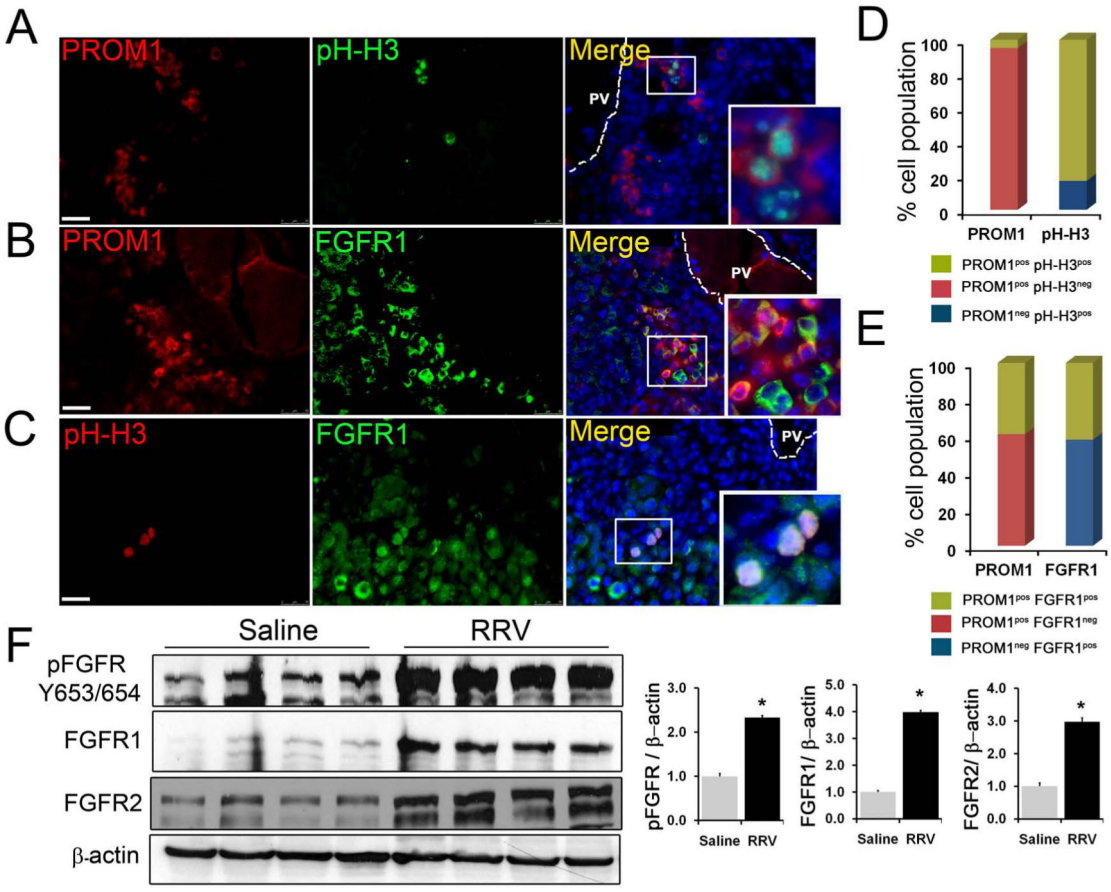

Figure 5.

Proliferation of PROM1^{pos} cells is associated with activated FGF signaling. (A-C) Immunofluorescence co-staining for PROM1 with proliferation marker, phospho-Histone H3 (pHH3) and FGF Receptor1 (FGFR1). Nuclei were stained with DAPI. Images represent three or more independent staining on 2-week saline and RRV BA livers. PV= portal vein. Scale bar=25μm. (D, E) Block diagram representing the percentage cell population (n=3-4). (F) Western blot analysis of protein extracts prepared from whole livers from 2-week saline control and RRV BA livers. n=4, p<0.0.005.

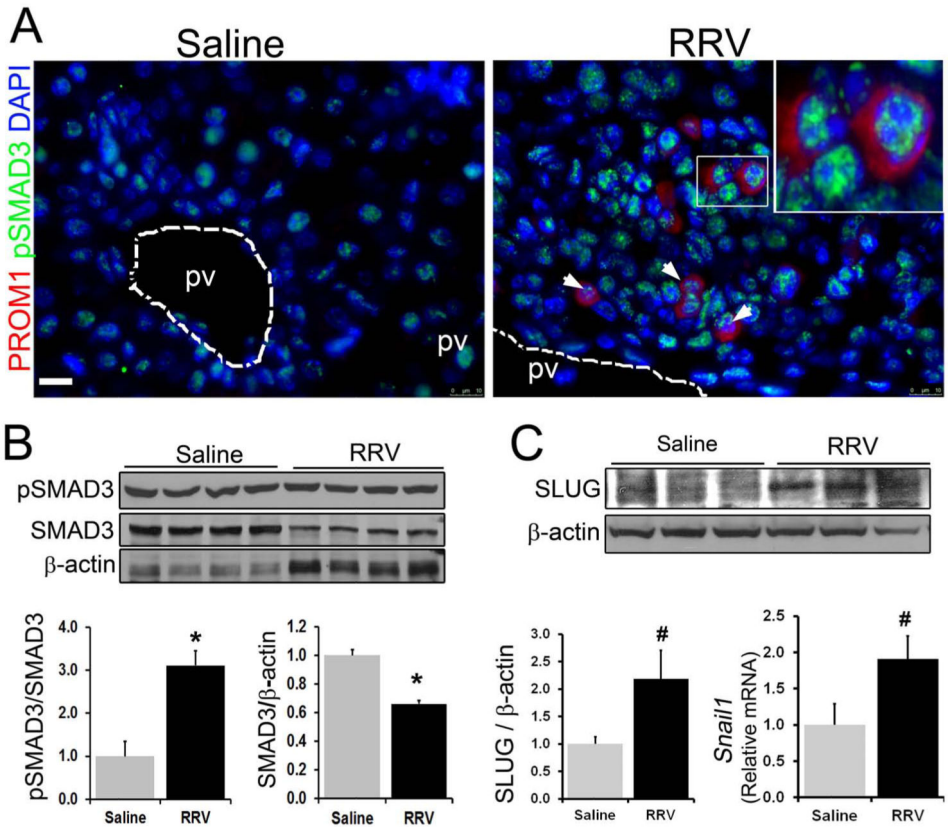

Figure 6.

Activation of TGFβ signaling in RRV BA livers. (A) Co-immunofluorescence staining of PROM1 with pSMAD3, downstream target of activated TGFβ signaling. Nuclei were stained with DAPI. Scale bar =25μm. Western blot analysis for (B) pSMAD3, SMAD3, and (C) SLUG in 2-week saline and RRV BA liver. (D) Quantitative PCR was performed to determine the expression level of *Snail*. n=4-6, **p*<0.005, # 0.05.

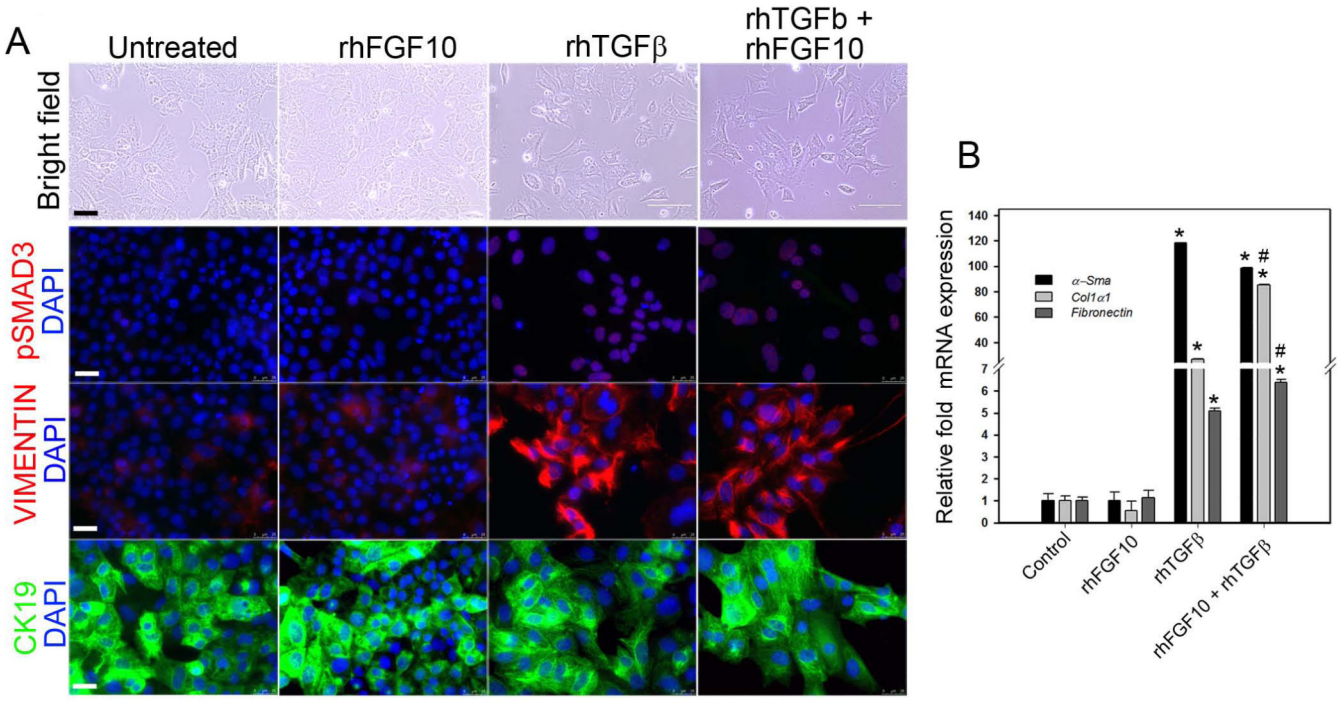

Figure 7.

TGFβ signaling induces myofibroblastic differentiation of PROM1-expressing HPCs *in vitro*. Serum starved *Mat1a*$^{-/-}$ PROM1 expressing hepatic progenitor cells were treated with recombinant human (rh) TGFβ and/or FGF10 for 3 days. Bright field images and immunofluorescence images for pSMAD3, VIMENTIN and CK19 were shown in (A). Images represent four independent experiments for each condition. Nuclei were stained with DAPI. Scale bar 25μm. (B) Gene expression analysis of *Mat1a*$^{-/-}$ cells by quantitative PCR. Treatment of TGFβ and FGF10+ TGFβ treatment resulted in a significant increased expression of fibrotic genes *Col1α1*, *αSma* and *Fibronectin* compared to control and rhFGF10 treated cells. (n=4, * p< 0001 compared to control and rhFGF10 treated. # p< 0.05 compared to TGFβ treated cells.

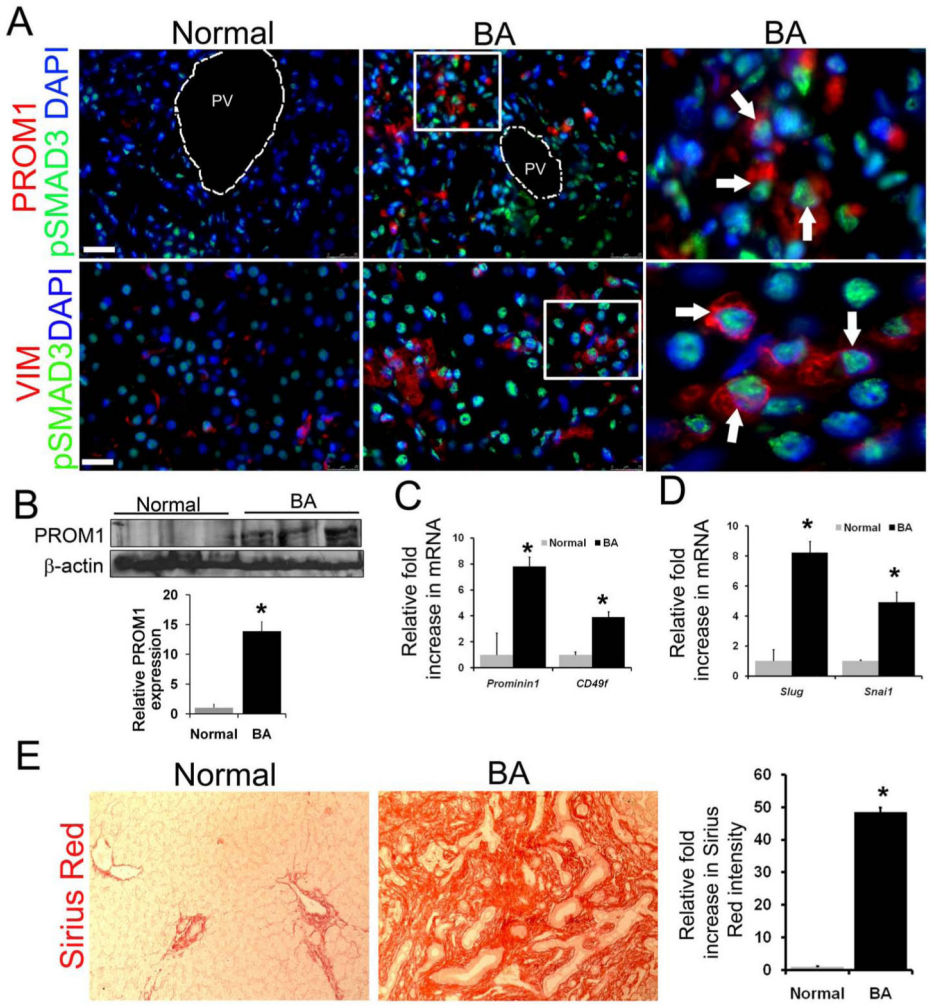

Figure 8.

Expansion of PROM1^{pos} cells with TGFβ activation in human BA livers. (A) Co-localization of PROM1^{pos} and VIMENTIN^{pos} cells with pSMAD3 in human BA biopsy samples received at the time of Kasai operation. Nuclei were stained with DAPI. Images are representative of analyses from 4-6 individual biopsy samples. Scale bar 25μm. (B) Expression level of PROM1 in human BA biopsy samples by Western blot analysis (n=3, * p< 0.01. (C) Quantitative PCR demonstrates increased expression level of downstream TGFβ signaling targets genes, *Slug* and *Snail* in BA livers compared to normal controls. (D) Quantitative PCR demonstrates increased expression level of *Prominin1* and *Cd49f* in BA livers compared to age matched normal controls, (n=4, BA=8 *p<0.01). (E) Sirius Red staining in normal and BA livers with densitometric quantification. All the BA tissues were received during Kasai operation. Median age of BA patients was 2 months. Age matched normal liver tissues were used as controls.(n=4, BA=7 * p<0.00001). Scale bar=25μm, PV= portal vein. Arrows indicate cells that co-express proteins on each panel.